Stokes *et al*. 10.1073/pnas.0707579104.

Supporting Information

Files in this Data Supplement:

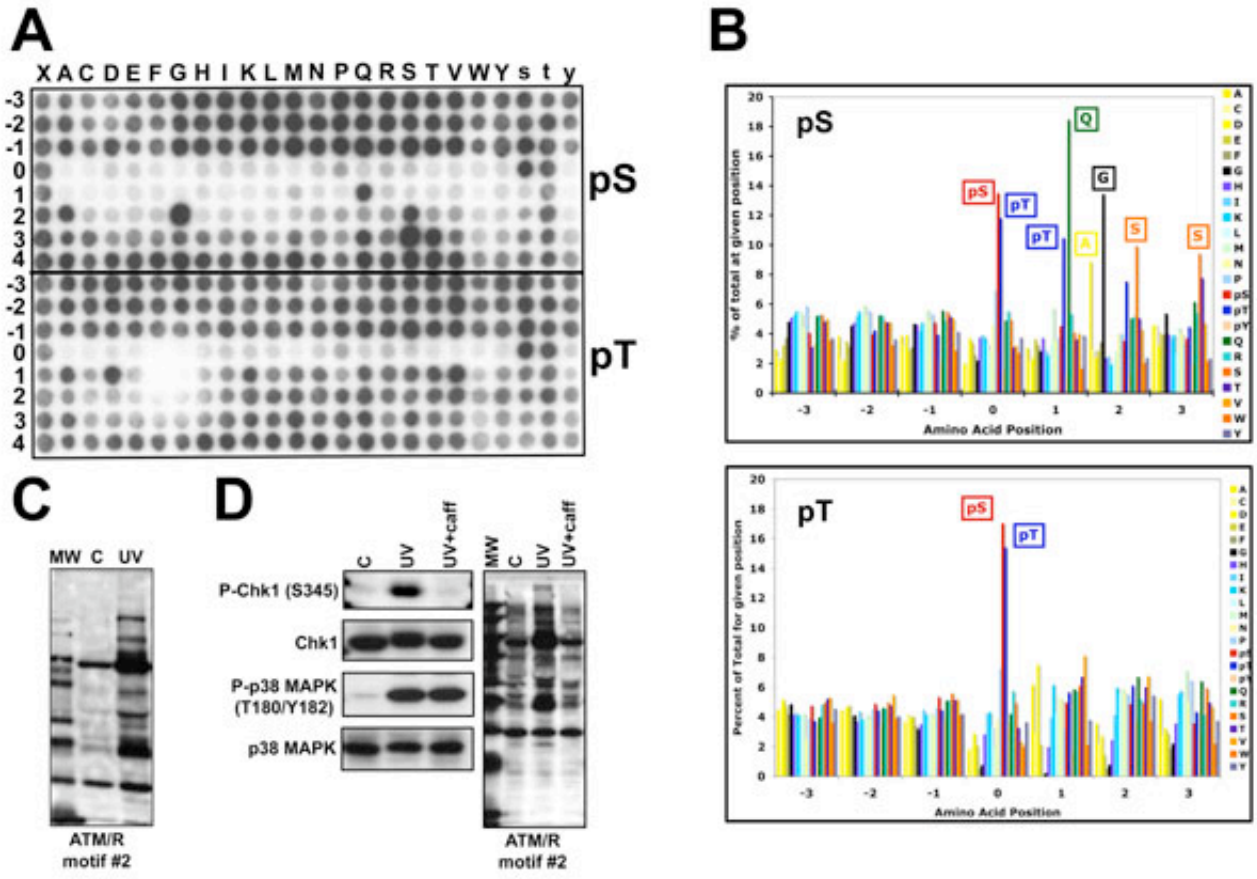

Fig. 4. Characterization of a novel ATM/R substrate motif antibody used in this study. (*A*) Peptide library array blot using ATM/R motif antibody-2. Peptides contained the minimum motif XXLS*QXXX (top half), or XXLT*QXXX (bottom half), where X is an equimolar mixture of all amino acids. Column 1 (X) for each row is the minimum motif, while following columns test addition of a fixed amino acid at the corresponding residue relative to the phosphorylation site. Letters above the blot denote the amino acid fixed at the corresponding position shown on the left. (*B*) Quantification of a digitized version of the peptide array blots using ATM/R motif antibody-2. The top half (fixed phosphoserine, pS), and bottom half (fixed phosphothreonine, pT) of the blot in *A* were graphed independently. For each position relative to pS or pT, the total intensity for all amino acids was added, and the percent intensity for each amino acid was calculated and plotted. Amino acids with a percentage more than two standard deviations from the mean are denoted with a box indicating the amino acid. (*C*) Phosphorylation of multiple bands in response to UV damage of DNA. Undamaged (*C*) or UV damaged (UV) M059K cell lysates were blotted with ATM/R motif antibody-2. (*D*) The phosphorylation seen with ATM/R motif antibody-2 after UV damage is caffeine sensitive. Undamaged (C), UV damaged (UV), or UV damaged + caffeine (UV + caff) M059K lysates were blotted with the indicated antibody.

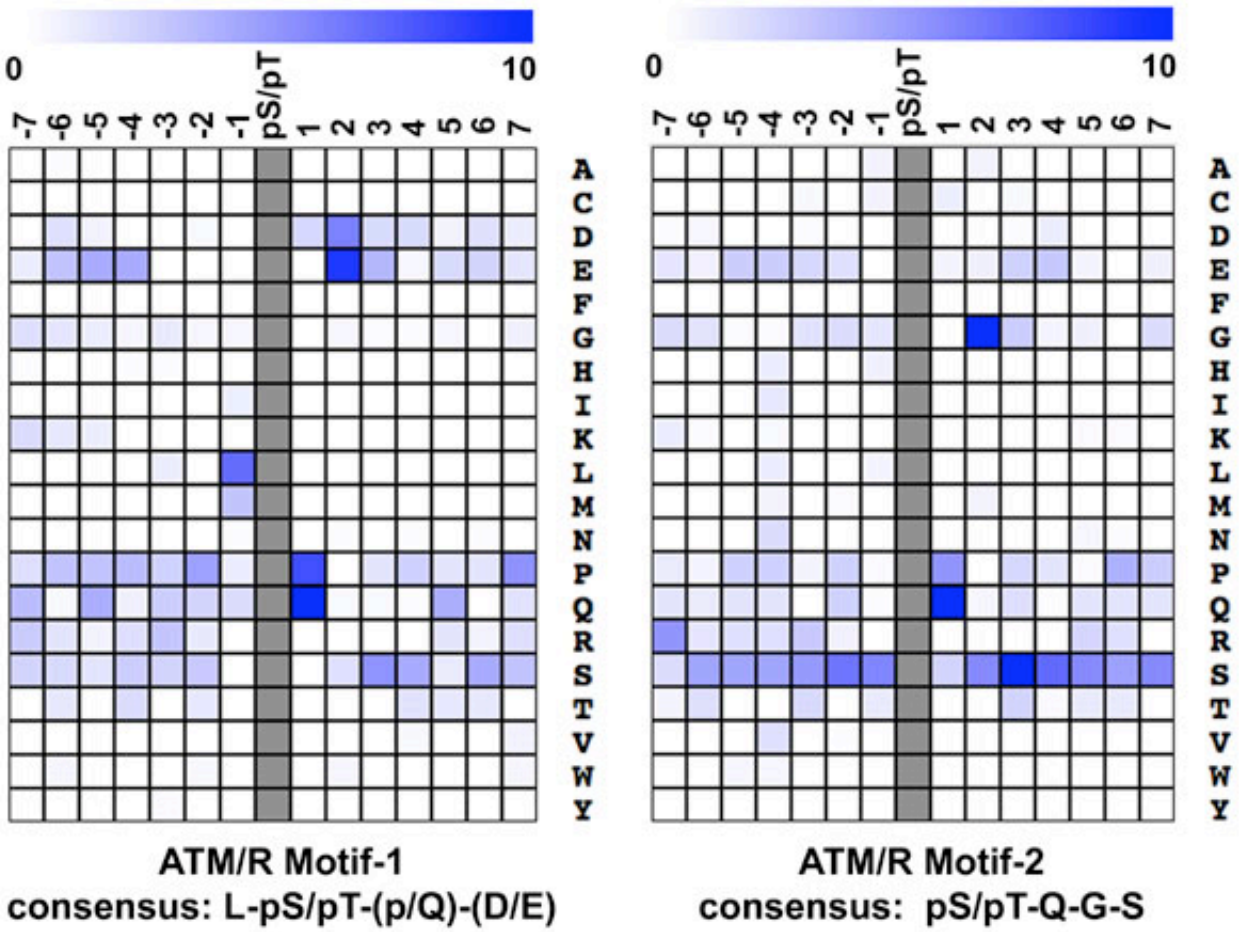

Fig. 5. Frequency maps of the data obtained for the two motif antibodies reveal differing substrate specificities. Relative abundance of each amino acid at residues surrounding the phosphorylation site is shown from low (white) to high (blue). The frequency map for ATM/R substrate motif antibody-1 is shown on the left, the map for ATM/R motif antibody-2 is shown on the right. A consensus sequence for each antibody is shown below the frequency map. A lowercase "p" in the consensus sequence for antibody-1 denotes a lesser preference for P than for Q at that position.

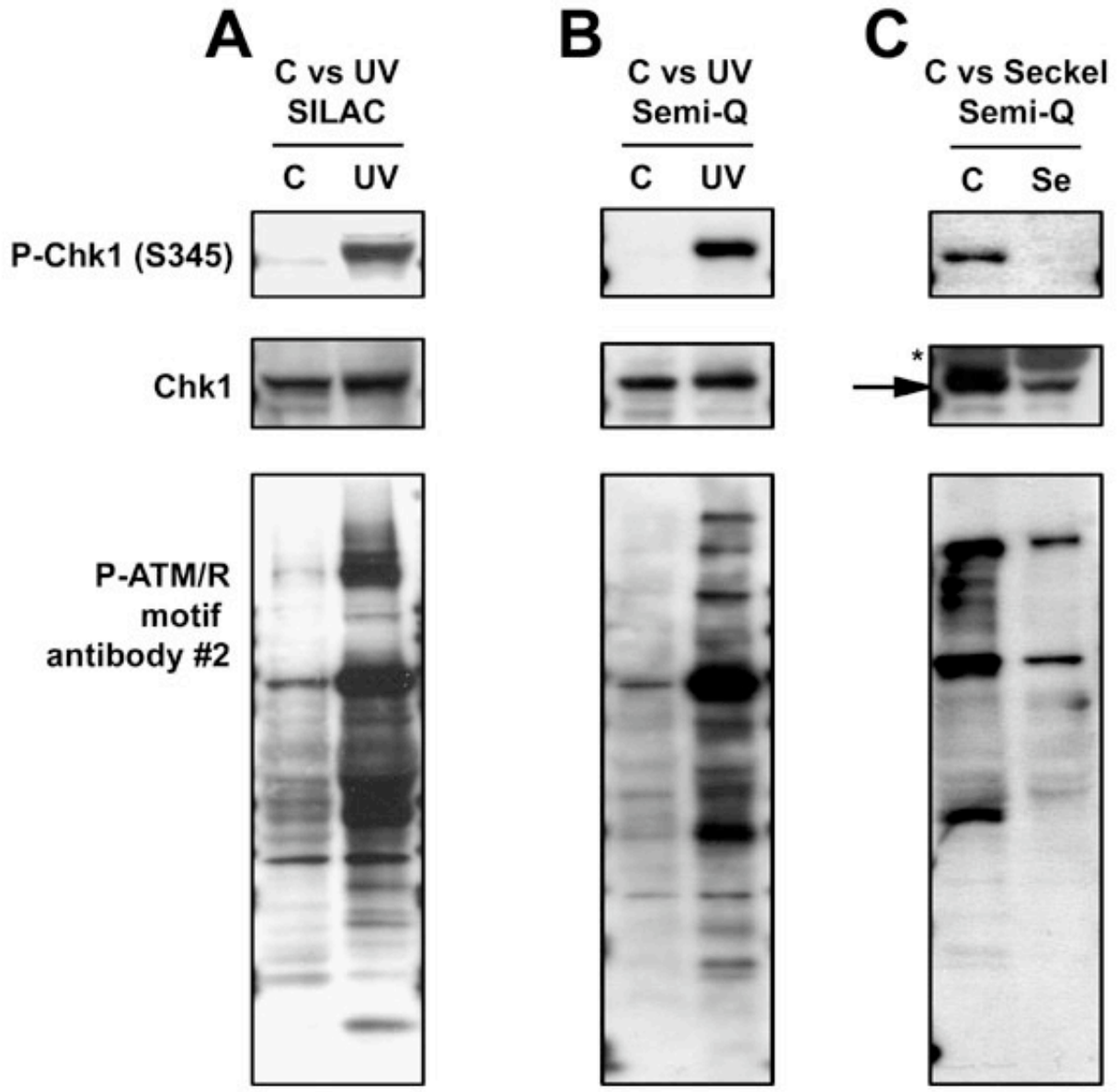

Fig. 6. Lysates used for immunoaffinity purification/LC-MS/MS analysis have a normal DNA damage response profile. (*A*) Western blotting analysis of undamaged (*C*) versus 50 mJ/cm^2, 2-hr rest UV damaged (UV) M059K cell lysates used for SILAC analysis. Samples for analysis were taken prior to mixing and trypsinization of light- (undamaged) and heavy-isotope labeled (UV damaged) lysates. Samples were probed with the indicated antibodies. (*B*) Western blotting analysis of undamaged (*C*) versus 50 mJ/cm^2, 2-hr rest UV damaged (UV) M059K cell lysates used for semiquantitative analysis. Samples for analysis were taken prior to trypsinization of lysates. Samples were probed with the indicated antibodies. (*C*) Western blotting analysis of lysates used for semiquantitative analysis of control cells (*C*) versus Seckel syndrome cells (Seckel), both UV damaged (50 mJ/cm^2, 2-hr rest). Samples for analysis were taken prior to trypsinization of lysates. Samples were probed with the indicated antibodies. An arrow denotes the Chk1 band in the Chk1 blot, while an asterisk (*) denotes a background band.

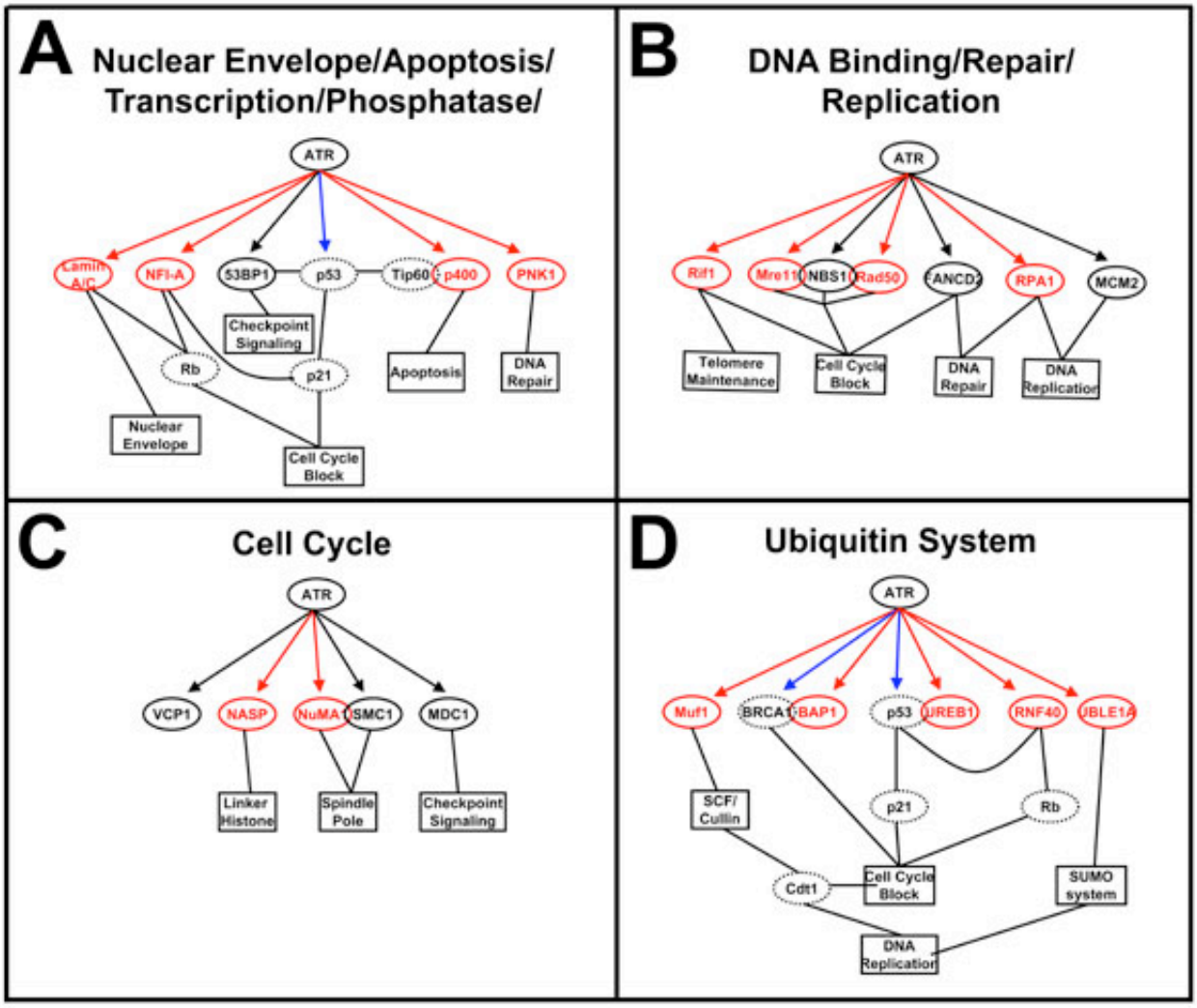

Fig. 7. Semiquantitative analysis of control vs. UV damaged M059K cells reveals diversity of known/novel substrates. (*A-D*) Pathway diagrams for proteins found in the semi-quantitative analysis for select protein classes [(*A*) Nuclear Envelope/Apoptosis/Transcription/ Phosphatase, (*B*) DNA-binding/repair/replication, (*C*) Cell cycle, and (*D*) Ubiquitin system]. Known phosphorylation events are shown in black, novel events are shown in red. Blue indicates a known phosphorylation that was not seen in the analysis. Proteins with a dashed outline were not seen in the analysis. Boxes denote cellular processes/localizations associated with the linked protein. Arrows connecting two proteins denote phosphorylation, lines denote interaction/regulation. Contact between two proteins signifies physical interaction. For each category, proteins shown are only those with potentially important links to cellular processes, not necessarily all the proteins from that category. For simplicity, only ATR is shown at the top of the pathway, though other DNA damage-activated kinases may also be responsible for the phosphorylation.

SI Text

Cell Culture/DNA Damage

M059K cells were maintained in DMEM supplemented with 10% FBS, 1 unit/ml penicillin G, and 1 mg/ml streptomycin. GM00200 and GM18366 cells were maintained in MEM supplemented with 1 mM sodium pyruvate, 10% FBS, 1 unit/ml penicillin G, and 1 mg/ml streptomycin. All cell lines were grown at 37°C with 5% CO_2. Cells were UV irradiated at 50 mJ/cm^2 in a Stratagene 2400 Stratalinker. After irradiation, cells were allowed to rest for 2 h before harvesting. Caffeine (USB, Cleveland, OH) was added at a final concentration of 2 mM to plates 10 min before treatment. UV treatment was as before, except that the rest period was only 1 h. For LC-MS/MS experiments, 2×10^8 cells were used for each sample. For all other experiments, 80% confluent 15-cm tissue culture plates were harvested with 500 ml of cell lysis buffer [20 mM Tris (pH 7.5), 150 mM NaCl, 1 mM EDTA, 1 mM EGTA, 1% Triton X-100, 2.5 mM sodium pyrophosphate, 1 mM beta-glycerophosphate, 1 mM Na_3VO_4, 1 mg/ml leupeptin], sonicated, and centrifuged at 14,000 rpm for 10 min. Protein concentrations were equalized by performing a Bradford assay and adjusting the concentrations with cell lysis buffer.

For SILAC experiments, M059K cells were grown in DMEM lacking arginine and lysine supplemented with 10% dialyzed FBS, 1 unit/ml penicillin G, 1 mg/ml streptomycin, and either 50 mg/ml L-lysine and 50 mg/ml L-arginine (light sample), or 50 mg/ml $^{13}C_6$ L-lysine, and 50 mg/ml $^{13}C_6$ L-arginine (Cambridge Isotope Labs, Andover, MA) (heavy sample). Cells were allowed to grow in their respective media for at least eight population doublings to ensure complete incorporation of heavy amino acids. Cells were treated (heavy cells with 50 mJ/cm^2 UV, 2 h rest, light cells untreated) and harvested as before. Total protein concentration of SILAC lysates for immunoaffinity purification/LC-MS/MS analysis was determined by Bradford assay, and concentrations of the heavy and light samples were adjusted to be equal with urea lysis buffer. Heavy and light samples were then mixed and used in PhosphoScan applications.

Immunoaffinity purification/LC-MS/MS

For each sample, 250 mg of ATM/R substrate motif antibody (Cell Signaling Technology) or phospho-Chk2 (T26/S28) antibody (ATM/R substrate motif antibody-2) (Cell Signaling Technology) were bound to 50 ml of Protein A Agarose beads (Roche Diagnostics, Indianapolis, IN) overnight at 4°C. Bead-antibody complexes were washed extensively in IAP buffer (see PhosphoScan Kit, Cell Signaling Technology, catalog #7900) before addition to peptide samples.

Immunoprecipitation eluates (100 ml) were concentrated and separated from antibody using Eppendorf PerfectPure C-18 Tips (Westbury, NY). Peptides were eluted from the microcolumn using 1 ml of 60% acetonitrile in 0.1% trifluoroacetic acid into 8 ml of 0.1% trifluoroacetic acid. Samples were run on a Thermo Electron LTQ ion trap mass spectrometer. Turbosequest (ThermoFinnigan) searches were performed against the NCBI Human database released on August 24, 2004 (containing 27,175 proteins) with serine or threonine phosphorylation (S + 80, T + 80) and oxidized methionine (M + 16) allowed as variable modifications. Peptides were score filtered using an XCorr cutoff of 1.5 for *z* of 1, 2.2 for z of 2, and 3.3 for *z* of 3 or more. Analytical replicates from one biological sample were run sequentially on the LC-MS/MS.

Semiquantitative Analysis

For each experiment, the immunoprecipitation eluates were split in half and analyzed in duplicate by LC-MS/MS, generating four analytical results: Two for control samples and two for either UV-treated or Seckel cell samples. For each analytical result, sequences were assigned to MS/MS spectra using the TurboSequest module of Proteomics Browser (ThermoFinnigan). During the process of extracting MS/MS files (DTA files) from a raw data file, TurboSequest generated an lcq_chro.txt file that related each MS/MS spectrum to the MS spectrum number, intensity, and retention time of its parent ion at its chromatographic apex. Thus, parent ion apex intensity for each Sequest assignment was measured automatically as part of the Sequest search process, and these intensities were used to reconstruct the chromatogram and as the basis for a label-free quantitative comparison of samples. The underlying parameters for peak picking and intensity measurement are built into Proteomics Browser and could not be configured; however, parent ion apex intensity for each peptide was manually checked in extracted ion chromatograms and either confirmed or corrected.

To simplify semiquantitative analysis, peak intensities were normalized by adjusting the intensity of one unchanged peptide ion in each sample set (four related analyses) to an arbitrary value of 1,000 and then scaling all other peptide ion intensities proportionally. For ATM/R substrate motif antibody-1 with control- and UV-treated cells and with control and Seckel cells, we used the Erk2 peptide (VADPDHDHTGFLT*EYVAT*R), charge of 3 for normalization; for ATM/R motif antibody-2 with control- and UV-treated cells, we used the periaxin peptide (MPS*LGIGVS*GPEVK), charge of 2; and for ATM/R motif antibody-2 with control and Seckel cells, we used the SH3 multiple domains 1 peptide (AAS*QGSDSPLLPAQR), charge of 2. After normalization, each sample in a sample set was compared and a fold-change was measured by taking the ratios of normalized intensities. In this manner semiquantitative analysis indicated in a non-rigorous manner where significant changes in phosphorylation levels might be occurring. These changes were verified by comparing the extracted ion chromatograms for that peptide ion to the extracted ion chromatograms for the peptide ions used for normalization. A 2-fold increase was considered significant based on statistical analysis. For peptides with measured intensities in both analytical replicates, the ratios between the two intensities were taken, and then these ratios were averaged. A two-fold change was outside the average ± 1 standard deviation and was therefore chosen as a minimum change for a significant intensity difference between samples. The average and standard deviation values are shown at the bottom of SI Tables 5 and 7.

SILAC

For each experiment, the immunoprecipitation eluates were split in half and analyzed in duplicate by LC-MS/MS, creating 4 data sets: 2 for control, and 2 for UV. Sequence result files (.srf files) were created and loaded into Bioworks Browser v.3.3 (ThermoElectron Corp.). SILAC ratios were calculated and exported to an Excel file. Peptides that fulfilled any of the following criteria were removed: Did not contain the minimum pSQ or pTQ motif, contained a mix of heavy and light lysine or arginine, or were only present as the light (undamaged) version of the peptide. Proper peak integration for each peptide was manually checked, and either manually adjusted (to accurately reflect integration of a single, clear peak) or discarded (if a peak assignment could not be made). For those peptides in which peak assignments could not be made in Bioworks Browser, extracted ion chromatograms were created in QualBrowser v.2.0 (ThermoElectron Corp.) to find either the ratio between peak intensities of the heavy and light versions of the peptide, or a ratio of the heavy version of the peptide to the background in the same m/z range. For peptides with measured intensities in both sample replicates, an average ratio was reported.

IP/Western

Two hundred micrograms of ATM/R substrate motif antibody or ATM/R substrate motif antibody-2 were coupled to 125 ml of packed Protein A Agarose beads overnight at 4°C. Beads were washed three times with 1 ml of PBS and twice with 1 ml of buffer CL (0.2 M triethanolamine, pH 8.2). Bead-antibody complexes were covalently coupled in 1 ml of buffer CL + 25 mM dimethyl pimelinediimidate dihydrochloride (DMP) (Sigma Aldrich, St. Louis, MO) for 1 h at room temperature. Beads were washed once with 1 ml of 0.1 M ethanolamine, pH 8.2, then incubated 1 h at room temperature with 1 ml of 0.1 M ethanolamine, pH 8.2. Beads were washed twice with 1 ml PBS and twice with 1 ml of 0.1 M glycine, pH 2.7. Beads were washed three times with 1 ml cell lysis buffer and used immediately.

One hundred twenty microliters of 50% bead slurry was incubated with 1 ml of cell lysate in cell lysis buffer overnight at 4°C. Supernatants were removed and mixed with SDS/PAGE loading dye [62.5 mM Tris-HCl (pH 6.8 at 25°C), 2% wt/vol SDS, 10% glycerol, 50 mM DTT, 0.01% wt/vol phenol red]. Beads were then washed three times with 1 ml of cell lysis buffer. Proteins were eluted with 100 ml of 0.1 M glycine, pH 2.7, in two 50-ml elution steps. Eluates were immediately neutralized with 8 ml of 1 M Tris, pH 8.0 and mixed with SDS/PAGE loading dye for Western blotting.

Discussion

We have hypothesized roles for some of the previously undescribed proteins found to be differentially phosphorylated in response to UV damage based on current literature to highlight potential links between previously undescribed proteins and DNA damage response or cell cycle signaling.

Nuclear Envelope/Apoptosis/Transcription/Phosphatase

Differential phosphorylation at SQ/TQ motifs was observed on some nuclear envelope associated proteins (SI Fig. 7*A*), which may provide new links by which ATM/R can signal to control such processes as nuclear import/export, and nuclear envelope breakdown in mitosis. One nuclear envelope protein found to be differentially phosphorylated, lamin A/C, associates with and stabilizes the tumor suppressor Rb, and its absence has been shown to cause defects in the response to ionizing radiation (1). Phosphorylation of lamin A/C may affect its role in the response to DNA damage, perhaps through increased stabilization of Rb.

Proteins involved in apoptotic reactions with increased phosphorylation after UV damage included p400, an E1A associated protein (SI Fig. 7*A*). p400 and its associated Tip60 are required for UV damage-mediated apoptosis. Tip60 stabilizes p53 (and acts as a coactivator after DNA damage), increasing transcription of p21 and proapoptotic genes. p400 normally inhibits this stabilization, however DNA damage abrogates this inhibition, leading to p21/apoptotic gene transcription (2). Phosphorylation of p400 at S2050 after DNA damage may be the event that causes the de-repression of Tip60 activity and resulting cell cycle blockage/apoptosis. This represents yet another connection by which the DNA damage checkpoint may signal to p53.

Several proteins involved in transcriptional regulation were found to contain differentially phosphorylated SQ/TQ motifs (SI Fig. 7*A*). For example, NFI-A is a transcriptional regulator responsible for repression of p21 expression (3). Phosphorylation of NFI-A could render it unable to repress p21 transcription, thus promoting p21-dependent cell cycle blockage in response to damage. Other transcriptional regulators such as 53BP1, which was also seen in the analysis, are known to be phosphorylated by ATM/R [although its function in checkpoint signaling is separate from its transcriptional activity (4)]. Although 53BP1 is a

known substrate of ATM/R, the phosphorylation sites found in this study are distinct from previously characterized sites.

Phosphatases found by semiquantitative analysis to be differentially phosphorylated included the DNA phosphatase PNK1 (SI Fig. 7*A*). PNK1 catalyzes both the 5'-phosphorylation and 3'-dephosphorylation of DNA ends. PNK1 has been implicated in the repair of DNA strand breaks, such as those caused by ionizing radiation or camptothecin (5). This is the first report of phosphorylation of Pnk1, within a cluster of five sites from T111 to S126, including two SQ sites at S114 and S126. It will be of interest to determine if these phosphorylation sites have an effect on damage-induced localization or activity of PNK1.

DNA Binding/Repair/Replication

Many proteins involved in DNA reactions (DNA binding, repair, and replication) were found to be differentially phosphorylated in UV treated cells (SI Fig. 7*B*). These included known phosphorylation sites, such as S343 of NBS1, S596 of FANCD2, and S957 and S966 of SMC1 (6, 7). Interestingly, even though many connections between ATM/R and DNA binding/repair/replication proteins have been made, the majority of the SQ/TQ phosphorylation sites found (30 of 39) were novel. This included novel sites on known ATM/R substrates, such as S58 of NBS1 and S358 of SMC1. Several phosphorylation sites were from proteins involved in the DNA damage response but not previously shown to be phosphorylated by ATM/R. This included T180 of RPA1, the large subunit of the eukaryotic single stranded binding protein. RPA2 has long been known to be a substrate of ATM/R (8), but RPA1 was only recently shown to be phosphorylated in response to DNA damage (9, 10). This work is the first demonstration of RPA1 phosphorylation in response to UV damage. Further, the site of phosphorylation was identified as T180, conflicting with previous reports that identify phosphorylation sites only within residues 112-163 and 569-600 (10). Phosphorylation of RPA1 at T180 in response to UV damage may affect its role in DNA replication, DNA repair, or in establishing checkpoint signaling.

All three members of the MRN complex (Mre11/Rad50/NBS1) were more highly phosphorylated in UV damaged cells. The MRN complex responds to double strand breaks, and has more recently been postulated to affect ATM/R activation/localization in response to damage (11, 12). Previously, only NBS1 was known to be a target of ATM/R in response to damage. Although Mre11 and Rad50 are known to be phosphorylated (13, 14), this work has identified the sites of damage-inducible phosphorylation as S676 for Mre11 and S635 for Rad50 (a known phosphorylation site, however not in the context of DNA damage). These damage-specific phosphorylation events may affect the function of the MRN complex in the DNA damage checkpoint or DNA repair.

Phosphorylation of the telomere maintenance protein Rif1 was also increased upon UV damage of DNA. In addition to its role in telomere maintenance, Rif1 has been shown to be involved in the DNA damage checkpoint. Rif1 co-localizes with other checkpoint proteins after damage, and its inhibition leads to defects in responding to DNA damage in S phase (15). The phosphorylation of Rif1 seen in this work at S1098 and T1518 may play a role in its function in the intraS phase checkpoint.

Cell Cycle

Novel sites that were differentially phosphorylated were also observed in cell cycle proteins (SI Fig. 4*C*). For example, MDC1 and VCP are known to be phosphorylated by ATM/R (16, 17). The sites on MDC1, however, are distinct from those previously reported (13, 18). These may represent important novel sites of ATM/R-dependent regulation of a protein known to be critical to function of the DNA damage checkpoint

(19, 20).

Another cell cycle protein found to contain differentially phosphorylated SQ/TQ sites was NuMA-1, which is involved in spindle pole reactions (21). NuMA-1 may therefore be important in establishing/maintaining a G2/M checkpoint. Phosphorylation of NASP, a chaperone for linker histone that is necessary for cell cycle progression (22), may lead to an inhibition of its function in driving cell cycle progression. Further study will be necessary to determine what role ATM/R-dependent phosphorylation plays in regulation of these cell cycle proteins and their associated cellular functions.

Ubiquitin System

Another class of proteins found to be differentially phosphorylated between undamaged and UV damaged M059K cells are associated with ubiquitin conjugation (SI Fig. 7*D*). ATR signaling has previously been linked to ubiquitination of target proteins, as in the monoubiquitination of FANCD2 (23). The DNA damage response has also been shown to modulate polyubiquitination, in which the end result is protein degradation, as with the DNA damage-induced destruction of the replication initiation factor Cdt1 (24, 25). RNF40 and UREB1 represent examples of potential novel ATM/R substrates among proteins in the ubiquitin system. RNF40, an E3 ubiquitin ligase, binds to both p53 and Rb, which are known cell cycle inhibitors (26, 27). Phosphorylation of RNF40 may alter its interaction with p53/Rb, perhaps potentiating their ability to block cell cycle progression. UREB1, another ubiquitin-protein ligase, ubiquitinates p53, and blocks p53 activity (28). Thus it is possible phosphorylation of UREB1 may inhibit its ability to negatively regulate p53. Muf1 was also seen in the analysis. This protein interacts with cullin/Rbx1 complexes, which block cell cycle progression through such mechanisms as destruction of Cdt1 (29). UBLE1A (also known as SAE1) is an E1 SUMO (small ubiquitin-like modifier) ligase. Phosphorylation of UBLE1A may affect protein sumoylation, which is known to regulate DNA damage responses (30).

BAP1, a protein known to interact with the checkpoint protein BRCA1 (31), was found to be phosphorylated in response to UV damage. BAP1 is a known ubiquitin hydrolase, although its targets are at this time not well understood. These novel phosphorylation events may modulate BAP1 activity or localization, impacting its role in the DNA damage response.

1. Johnson BR, Nitta RT, Frock RL, Mounkes L, Barbie DA, Stewart CL, Harlow E, Kennedy BK (2004) *Proc Natl Acad Sci USA* 101:9677-9682.

2. Tyteca S, Vandromme M, Legube G, Chevillard-Briet M, Trouche D (2006) *EMBO J* 25:1680-1689.

3. Ouellet S, Vigneault F, Lessard M, Leclerc S, Drouin R, Guerin SL (2006) *Nucleic Acids Res* 34:6472-6487.

4. Adams MM, Carpenter PB (2006) *Cell Div* 1:19.

5. Jilani A, Ramotar D, Slack C, Ong C, Yang XM, Scherer SW, Lasko DD (1999) *J Biol Chem* 274:24176-24186.

6. Ho GP, Margossian S, Taniguchi T, D'Andrea AD (2006) *Mol Cell Biol* 26:7005-7015.

7. Traven A, Heierhorst J (2005) *Bioessays* 27:397-407.

8. Zou Y, Liu Y, Wu X, Shell SM (2006) *J Cell Physiol* 208:267-273.

9. Patrick SM, Oakley GG, Dixon K, Turchi JJ (2005) *Biochemistry* 44:8438-8448.

10. Nuss JE, Patrick SM, Oakley GG, Alter GM, Robison JG, Dixon K, Turchi JJ (2005) *Biochemistry* 44:8428-8437.

11. Zhou J, Lim CU, Li JJ, Cai L, Zhang Y (2006) *Cancer Lett* 243:9-15.

12. Kim JE, Minter-Dykhouse K, Chen J (2006) *Mol Carcinog* 45:403-408.

13. Beausoleil SA, Jedrychowski M, Schwartz D, Elias JE, Villen J, Li J, Cohn MA, Cantley LC, Gygi SP (2004) *Proc Natl Acad Sci USA* 101:12130-12135.

14. Dong Z, Zhong Q, Chen PL (1999) *J Biol Chem* 274:19513-19516.

15. Silverman J, Takai H, Buonomo SB, Eisenhaber F, de Lange T (2004) *Genes Dev* 18:2108-2119.

16. Goldberg M, Stucki M, Falck J, D'Amours D, Rahman D, Pappin D, Bartek J, Jackson SP (2003) *Nature* 421:952-956.

17. Livingstone M, Ruan H, Weiner J, Clauser KR, Strack P, Jin S, Williams A, Greulich H, Gardner J, Venere M, *et al.* (2005) *Cancer Res* 65:7533-7540.

18. Olsen JV, Blagoev B, Gnad F, Macek B, Kumar C, Mortensen P, Mann M (2006) *Cell* 127:635-648.

19. Peng A, Chen PL (2005) *Cancer Res* 65:1158-1163.

20. Stewart GS, Wang B, Bignell CR, Taylor AM, Elledge SJ (2003) *Nature* 421:961-966.

21. Sun QY, Schatten H (2006) *Front Biosci* 11:1137-1146.

22. Richardson RT, Alekseev OM, Grossman G, Widgren EE, Thresher R, Wagner EJ, Sullivan KD, Marzluff WF, O'Rand MG (2006) *J Biol Chem* 281:21526-21534.

23. Andreassen PR, D'Andrea AD, Taniguchi T (2004) *Genes Dev* 18:1958-1963.

24. Higa LA, Mihaylov IS, Banks DP, Zheng J, Zhang H (2003) *Nat Cell Biol* 5:1008-1115.

25. Kondo T, Kobayashi M, Tanaka J, Yokoyama A, Suzuki S, Kato N, Onozawa M, Chiba K, Hashino S, Imamura M, *et al.*(2004) *J Biol Chem* 279:27315-27319.

26. Kim J, Hake SB, Roeder RG (2005) *Mol Cell* 20:759-770.

27. Wen H, Ao S (2000) *Biochem Biophys Res Commun* 275:141-148.

28. Yoon SY, Lee Y, Kim JH, Chung AS, Joo JH, Kim CN, Kim NS, Choe IS, Kim JW (2005) *Biochem Biophys Res Commun* 326:7-17.

29. Kamura T, Burian D, Yan Q, Schmidt SL, Lane WS, Querido E, Branton PE, Shilatifard A, Conaway RC, Conaway JW (2001) *J Biol Chem* 276:29748-29753.

30. Muller S, Ledl A, Schmidt D (2004) *Oncogene* 23:1998-2008.

31. Jensen DE, Proctor M, Marquis ST, Gardner HP, Ha SI, Chodosh LA, Ishov AM, Tommerup N, Vissing H, Sekido Y, *et al.* (1998) *Oncogene* 16:1097-1112.